

Production of the Exotic 1^{--} Hadrons $\phi(2170)$, $X(4260)$, and $Y_b(10890)$ at the LHC and Tevatron via the Drell-Yan Mechanism

Ahmed Ali* and Wei Wang†

Deutsches Elektronen-Synchrotron DESY, D-22607 Hamburg, Germany

(Received 24 March 2011; published 11 May 2011)

We calculate the Drell-Yan production cross sections and differential distributions in the transverse momentum and rapidity of the $J^{PC} = 1^{--}$ exotic hadrons $\phi(2170)$, $X(4260)$, and $Y_b(10890)$ at the LHC and the Tevatron. These hadrons are tetraquark (four-quark) candidates, with a hidden $s\bar{s}$, $c\bar{c}$, and $b\bar{b}$ quark pair, respectively. In deriving the distributions, we include the order α_s QCD corrections, resum the large logarithms in the small transverse momentum region in the impact-parameter formalism, and use the state of the art parton distribution functions. Production rates for the processes $pp(\bar{p}) \rightarrow \phi(2170) \times (\rightarrow \phi(1020)\pi^+\pi^- \rightarrow K^+K^-\pi^+\pi^-) + \dots$, $pp(\bar{p}) \rightarrow X(4260) (\rightarrow J/\psi\pi^+\pi^- \rightarrow \mu^+\mu^-\pi^+\pi^-) + \dots$, and $pp(\bar{p}) \rightarrow Y_b(10890) (\rightarrow Y(1S, 2S, 3S)\pi^+\pi^- \rightarrow \mu^+\mu^-\pi^+\pi^-) + \dots$ are presented. Their measurements will help in understanding the dynamics of these exotic hadrons.

DOI: 10.1103/PhysRevLett.106.192001

PACS numbers: 14.40.Rt, 13.85.Ni

Exotic hadron spectroscopy now stands on firm footing, thanks mainly to experiments during the last several years at the two e^+e^-B factories, *BABAR*, and *Belle*, which have reported an impressive number of such states in the mass region of the charmonia [1]. Most of these states defy a conventional $c\bar{c}$ charmonium interpretation, but their affinity to decay into the hidden charm states J/ψ , ψ' and into open charm states $D\bar{D}^{(*)}$ reveal that they have a $c\bar{c}$ component in their Fock space. Of particular interest for us is the $J^{PC} = 1^{--}$ state $Y(4260)$, discovered by *BABAR* [2] in the initial state radiation (ISR) process $e^+e^- \rightarrow \gamma_{\text{ISR}}Y(4260) \rightarrow \gamma_{\text{ISR}}J/\psi\pi^+\pi^-$, confirmed later by *CLEO* [3] and *Belle* [4], with the latter finding that two interfering Breit-Wigner amplitudes to the $J/\psi\pi^+\pi^-$ state describe the data better. Maiani *et al.* [5] have interpreted $Y(4260)$ as the first orbital excitation of a diquark-antidiquark (tetraquark) state ($[cs][\bar{c}\bar{s}]$). Particle Data Group (PDG) [6] has assigned the name $X(4260)$ for this resonance, which is what we also use.

Evidence exists also for an $s\bar{s}$ state $Y_s(2175)$ with the quantum numbers $J^{PC} = 1^{--}$, which was first observed by *BABAR* [7] in the ISR process $e^+e^- \rightarrow \gamma_{\text{ISR}}f_0(980)\phi(1020)$, where $f_0(980)$ is an 0^{++} scalar state, later confirmed by *BESII* [8] and *Belle* [9]. In [10], $Y_s(2175)$ is interpreted as a tetraquark $[sq][\bar{s}\bar{q}]$ with one unit of relative angular momentum. This state is now called $\phi(2170)$ by PDG [6], which we also use. Likewise, *Belle* [11,12] measured the state $Y_b(10890)$ in the process $e^+e^- \rightarrow Y_b(10890) \rightarrow Y(1S, 2S, 3S)\pi^+\pi^-$, which is interpreted as a hidden $b\bar{b}$ tetraquark state [13–15].

The aim of this Letter is to investigate the Drell-Yan production of the $J^{PC} = 1^{--}$ exotic hadrons at the Tevatron and the LHC $p\bar{p}(p) \rightarrow \gamma^* \rightarrow V + \dots$, with V being one of the states $\phi(2170)$, $X(4260)$, or $Y_b(10890)$. The running common thread is that all three are candidates for the first orbital excitation of diquark-antidiquark states

with a hidden $s\bar{s}$, $c\bar{c}$, and $b\bar{b}$ quark content, respectively. Drell-Yan processes are theoretically better understood than the corresponding hadronic (prompt) production processes. Unfortunately, due to the very small leptonic branching ratios [6], production of these exotic states in the traditional $\ell^+\ell^-$ pair ($\ell^\pm = e^\pm, \mu^\pm$) is not promising in the processes $p\bar{p}(p) \rightarrow \gamma^* \rightarrow V(\rightarrow \ell^+\ell^-) + \dots$.

We point out that the corresponding production cross sections are large enough to be measured at the LHC and the Tevatron, if, instead of the lepton pair, one concentrates on the final states in which these exotic vector hadrons have been discovered in the e^+e^- annihilation experiments: $\phi(2170) \rightarrow \phi(1020)f_0(980)$, $X(4260) \rightarrow J/\psi\pi^+\pi^-$, and $Y_b(10890) \rightarrow Y(1S, 2S, 3S)\pi^+\pi^-$. The obvious advantage is that the essential input (branching ratios for the discovery channels times the respective leptonic widths) needed for estimating the cross sections, are all provided by the e^+e^- experiments, yielding model-independent cross sections irrespective of the nature of these states. On the other hand, these measurements are challenging due to the preponderance of the $\pi^+\pi^-$ pairs from the underlying event in pp and $p\bar{p}$ collisions, and hence the combinatorial background is expected to be formidable. However, we trust that, once the energy-momentum profile of the background $\pi^+\pi^-$ pairs at the hadron colliders is well understood, the background can be effectively removed by appropriate cuts, enabling the experiments in carrying out significant measurements in this sector.

The Drell-Yan cross sections are based on the factorization theorem (here X denotes a bunch of hadrons)

$$\sigma(pp/p\bar{p} \rightarrow V + X) = \int dx_1 dx_2 \sum_{a,b} f_a(x_1) f_b(x_2) \times \sigma(a + b \rightarrow V(p) + X), \quad (1)$$

where a, b denotes a generic parton inside a proton or antiproton, $V = \phi(2170), X(4260), Y_b(10890)$ for the processes considered here with $p = (p^0, \vec{p}_T, p^3)$ being the momentum 4-vector of the V , and $f_a(x_1), f_b(x_2)$ are the parton distribution functions (PDFs), which depend on the fractional momenta $x_i (i = 1, 2)$ (an additional scale dependence is suppressed here). We shall adopt the MSTW (Martin-Stirling-Thorne-Watt) PDFs [16] in our numerical calculations, and use another PDF set, the CTEQ10 [17], to estimate the uncertainties from this source. The process-dependent partonic cross sections $\sigma(a + b \rightarrow V + X)$ will be computed using the QCD perturbation theory.

We recall that the leading order contribution comes from the subprocess $\bar{q}q \rightarrow \gamma^* \rightarrow V$

$$\sigma_0 = (\delta_{aq}\delta_{b\bar{q}} + \delta_{a\bar{q}}\delta_{bq}) \frac{\pi |g_{q\bar{q}V}|^2}{N_c} \delta(p^2 - m_V^2), \quad (2)$$

with $N_c = 3$. We include the leading order QCD [i.e., $O(\alpha_s)$] corrections, implemented following the pioneering papers [18,19]. This formalism is applied to calculate the differential distributions $d^2\sigma/dydp_T^2$, with the rapidity defined as $y \equiv \frac{1}{2} \ln \frac{p^0 + p^3}{p^0 - p^3}$. The transverse momentum distribution at the tree level has the form $\delta(p_T^2)$. Perturbative QCD (gluon bremsstrahlung) generates a nontrivial p_T distribution. However, large logarithms of the type $\alpha_s^n \ln^m(p^2/p_T^2)$ arising from higher order QCD corrections spoil the perturbative expansion in the small transverse momentum region. These large logarithms must be resummed in order to improve the convergence of the perturbation theory. This is done in the Collins-Soper-Sterman (CSS) framework [20] where the resummation is carried out in the impact-parameter space, yielding a simple form for the resummed p_T distribution

$$\frac{d^2\sigma}{dydp_T^2} = \frac{d^2\sigma^{\text{per}}}{dydp_T^2} + f(p_T) \left(\frac{d^2\sigma^{\text{res}}}{dydp_T^2} - \frac{d^2\sigma^{\text{asy}}}{dydp_T^2} \right), \quad (3)$$

in which $d^2\sigma^{\text{res}}/dydp_T^2$ reorganizes the singular terms in the $p_T \rightarrow 0$ limit. Explicitly, this takes the form

$$\begin{aligned} \frac{d^2\sigma^{\text{res}}}{dydp_T^2} &= \frac{\pi^2}{3s} \int \frac{d^2\vec{b}}{(2\pi)^2} e^{i\vec{p}_T \cdot \vec{b}} \sum_q g_{q\bar{q}V}^2 \\ &\times \sum_{a,b} \int_{x_1^0}^1 \frac{dx_1}{x_1} f_a(x_1, \mu) C_{qa/\bar{q}a} \left(\frac{x_1^0}{x_1}, \mu, g_s, \frac{c}{b} \right) \\ &\times \int_{x_2^0}^1 \frac{dx_2}{x_2} f_b(x_2, \mu) C_{\bar{q}b/qb} \left(\frac{x_2^0}{x_2}, \mu, g_s, \frac{c}{b} \right) \\ &\times \exp \left\{ -W \left(b, \frac{c}{b}, m_V, x_1, x_2 \right) \right\}, \quad (4) \end{aligned}$$

with $x_1^0 = m_V/\sqrt{s}e^y$, $x_2^0 = m_V/\sqrt{s}e^{-y}$, and s is the square of the center-of-mass collision energy. The function $f(p_T)$ in (3) is introduced as a matching function for which we use $f(p_T) = 1/[1 + (p_T/Q_{\text{match}})^4]$ [21]. To estimate the

uncertainty in the transverse momentum distributions caused by the matching procedure, we shall take $Q_{\text{match}} = (2 \pm 1)m_V$.

The Sudakov factor $W(b, \frac{c}{b}, p, x_1, x_2)$ is expressed as

$$W \left(b, \frac{c}{b}, p, x_1, x_2 \right) = \int_{c^2/b^2}^{p^2} \frac{d\bar{\mu}^2}{\bar{\mu}^2} \left[\ln \frac{p^2}{\bar{\mu}^2} A(g_s(\bar{\mu})) + B(g_s(\bar{\mu})) \right],$$

and the coefficient functions $A, B, C_{qa/\bar{q}a}(x_1^0/x_1)$, and $C_{\bar{q}b/qb}(x_2^0/x_2)$ are expanded [in units of $(\alpha_s/\pi)^{(n)}$]. Some leading terms in these expansions are [20]

$$\begin{aligned} A^{(1)} &= 4/3, & B^{(1)} &= -2, \\ C_{jk}^{(0)} &= \delta_{jk} \delta(1-z), & C_{jg}^{(1)} &= \frac{1}{2} z(1-z), \quad (5) \end{aligned}$$

$$C_{jk}^{(1)} = \delta_{jk} \left[\frac{2}{3}(1-z) + \delta(1-z) \left(\frac{\pi^2}{3} - \frac{8}{3} \right) \right],$$

where the integration constants C_1, C_2 in the Sudakov factor (not shown explicitly) and the renormalization scale μ in (4) have been taken as $C_1 = \mu b = c = 2e^{-\gamma_E}$ and $C_2 = 1$, where $\gamma_E = 0.57722$ is the Euler constant.

The asymptotic term in (3) coincides with the perturbative results in the small p_T region

$$\frac{d^2\sigma^{\text{asy}}}{dydp_T^2} = \frac{d^2\sigma^{\text{per}}}{dydp_T^2} \Big|_{p_T^2 \rightarrow 0}, \quad (6)$$

so that in this region the resummed terms dominate. The factorization scale is chosen as $\mu = \sqrt{p_T^2 + m_V^2}$.

As the large impact parameter b corresponds to a low momentum scale, a cutoff is introduced in the CSS formalism [20], which replaces the parameter b by $b^* = b/\sqrt{1 + b^2/b_{\text{max}}^2}$, with b_* bounded from above by b_{max} . The nonperturbative effects to compensate this cutoff are incorporated into a phenomenological function $F_{\text{NP}}(b, m_V, x_1, x_2)$, and a commonly adopted parametrization obtained by fitting the data on W and Z production [22] is given by

$$F_{\text{NP}} = \exp \left[-g_1 b^2 - g_2 b^2 \ln \frac{m_V}{2Q_0} - g_1 g_3 b \ln \left(\frac{x_1 x_2}{0.01} \right) \right],$$

where $g_1 = 0.11 \text{ GeV}^2$, $g_2 = 0.58 \text{ GeV}^2$, $g_3 = -1.5 \text{ GeV}^{-1}$, and $Q_0 = 1.6 \text{ GeV}$ for $b_{\text{max}} = 0.5 \text{ GeV}^{-1}$. It should be pointed out that the above value of Q_0 is not appropriate for $\phi(2170)$, as in this case $m_{\phi(2170)} < 2Q_0$, which would lead to an enhancement of the large b region instead of suppressing it, and therefore in our calculation we use as input $Q_0 = 1.0 \text{ GeV}$, which we adopt for the $Y_b(10890)$ and $X(4260)$ cases as well.

The electromagnetic coupling constants $g_{q\bar{q}V}$ are related to the e^+e^-V coupling g_{eeV} by $g_{q\bar{q}V} = e_q g_{eeV}$. The relevant e^+e^- experimental data which are used to derive these parameters are collected in Table I. The entries for $\Gamma_{ee}(Y_b)\mathcal{B}(Y_b \rightarrow Y(nS)\pi^+\pi^-)$ are obtained by

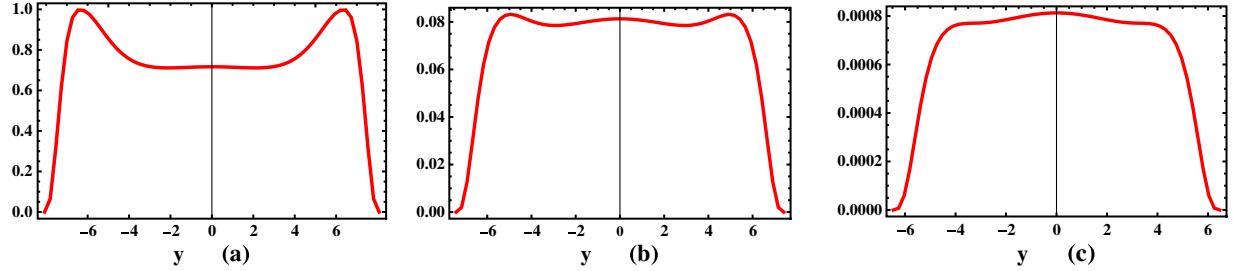


FIG. 1 (color online). Rapidity distributions $\frac{d\sigma}{dy}$ (in units of pb) for the process (a) $pp \rightarrow (\phi(2170) \rightarrow \phi(1020)f_0(980) \rightarrow K^+K^-\pi^+\pi^-) + \dots$, (b) $pp \rightarrow (X(4260) \rightarrow J/\psi\pi^+\pi^- \rightarrow \mu^+\mu^-\pi^+\pi^-) + \dots$, and (c) $pp \rightarrow (Y_b(10890) \rightarrow Y(1S, 2S, 3S)\pi^+\pi^- \rightarrow \mu^+\mu^-\pi^+\pi^-) + \dots$ at LHC with $\sqrt{s} = 7$ TeV using the MSTW PDFs.

using the relation $\Gamma_{ee}(Y_b)\mathcal{B}(Y_b \rightarrow Y(nS)\pi^+\pi^-) = \Gamma_{Y_b} m_{Y_b}^2 \sigma(Y(nS)\pi^+\pi^-)/(12\pi)$, with all three quantities on the right-hand side taken from Belle [12].

Having specified the formalism and the necessary inputs, we present our numerical results. As the distributions at the Tevatron and the LHC are rather similar, we show the figures only for the LHC. Rapidity distributions $d\sigma/dy$ (in units of pb) for the three Drell-Yan processes at the LHC for $\sqrt{s} = 7$ TeV are shown in Fig. 1: (a) $pp \rightarrow (\phi(2170) \rightarrow \phi(1020)f_0(980) \rightarrow K^+K^-\pi^+\pi^-) + \dots$, (b) $pp \rightarrow (X(4260) \rightarrow J/\psi\pi^+\pi^- \rightarrow \mu^+\mu^-\pi^+\pi^-) + \dots$, and (c) $pp \rightarrow (Y_b(10890) \rightarrow Y(1S, 2S, 3S)\pi^+\pi^- \rightarrow \mu^+\mu^-\pi^+\pi^-) + \dots$ (contributions from three intermediate states have been added). The normalized distributions are stable, though the indicated uncertainties in the normalization in Table II discussed below will also reflect in the rapidity distributions shown in this figure. The corresponding transverse momentum distributions $d\sigma/dp_T$ (in units of pb/GeV) are shown in Fig. 2, which are obtained for the rapidity range $|y| < 2.5$ (for ATLAS and CMS). The corresponding distributions in the rapidity range $1.9 < y < 4.9$ (for the LHCb) are very similar, and hence not

TABLE I. Masses, total, and partial decay widths of the $\phi(2170)$, $X(4260)$, and $Y_b(10890)$. Unless specified, all input values are taken from the PDG review [6].

	m_V (MeV)	Γ (MeV)	$\Gamma_{ee}\mathcal{B}$ (eV)
$\phi(2170)$	2175 ± 15	61 ± 18	2.5 ± 0.9^a
$X(4260)$	4263_{-9}^{+8}	108 ± 21 [4]	$6.0_{-1.3}^{+4.9}{}^b$ [4]
$Y_b(10890)$	$10888.4_{-2.9}^{+3.0}$ [12]	$30.7_{-7.7}^{+8.9}$ [12]	$0.69_{-0.20}^{+0.23}{}^c$ [12]
$\mathcal{B}_{\phi \rightarrow K^+K^-}$	$(48.9 \pm 0.5)\%$	$\mathcal{B}_{f_0(980) \rightarrow \pi^+\pi^-}$	$(50_{-9}^{+7})\%$ [23]
$\mathcal{B}_{J/\psi \rightarrow \mu^+\mu^-}$	$(5.93 \pm 0.06)\%$	$\mathcal{B}_{Y(1S) \rightarrow \mu^+\mu^-}$	$(2.48 \pm 0.05)\%$
$\mathcal{B}_{Y(2S) \rightarrow \mu^+\mu^-}$	$(1.93 \pm 0.17)\%$	$\mathcal{B}_{Y(3S) \rightarrow \mu^+\mu^-}$	$(2.18 \pm 0.21)\%$

^a $\Gamma_{ee} \times \mathcal{B}(\phi(2170) \rightarrow \phi(1020)f_0(980))$.

^b $\Gamma_{ee} \times \mathcal{B}(X(4260) \rightarrow J/\psi\pi^+\pi^-)$, corresponding to solution I.

^c $\Gamma_{ee} \times \mathcal{B}(Y_b(10890) \rightarrow Y(1S)\pi^+\pi^-)$ obtained from $\sigma = (2.78_{-0.41}^{+0.48})$ pb. For $Y_b \rightarrow Y(2S)\pi^+\pi^-$, the cross section $(4.82_{-0.91}^{+1.01})$ pb gives $\Gamma_{ee}\mathcal{B} = (1.20_{-0.37}^{+0.43})$ eV, while for $Y_b \rightarrow Y(3S)\pi^+\pi^-$, the cross section $(1.71_{-0.39}^{+0.42})$ pb corresponds to $\Gamma_{ee}\mathcal{B} = (0.42_{-0.14}^{+0.16})$ eV.

shown. The uncertainties caused by the matching functions are displayed.

The integrated cross sections for the processes $pp(\bar{p}) \rightarrow Y_b(10890)(\rightarrow Y(1S, 2S, 3S)\pi^+\pi^- \rightarrow \mu^+\mu^-\pi^+\pi^-) + \dots$, $pp(\bar{p}) \rightarrow X(4260)(\rightarrow J/\psi\pi^+\pi^- \rightarrow \mu^+\mu^-\pi^+\pi^-) + \dots$, and $pp(\bar{p}) \rightarrow \phi(2170)(\rightarrow \phi(1020)f_0(980) \rightarrow K^+K^-\pi^+\pi^-) + \dots$ at the Tevatron ($\sqrt{s} = 1.96$ TeV) and the LHC (for $\sqrt{s} = 7$ TeV and 14 TeV) are presented in Table II, using the MSTW PDFs [16]. The errors shown are from the parametric uncertainties in the PDFs and the various experimental inputs given in Table I, which we have added in quadrature. We have also checked that our results are modified only moderately if we use a different set of PDFs. For the CTEQ10 PDFs [17], most changes amount to less than 30%, which are smaller than the uncertainties from the experimental input. We remark that the cross sections for CDF and D0 ($\sqrt{s} = 1.96$ TeV) and the LHCb (for $\sqrt{s} = 7$ TeV) are comparable, despite different center-of-mass energies, due to their different rapidity ranges, whereas the cross sections for the ATLAS and CMS detectors at the LHC ($\sqrt{s} = 7$ TeV) are larger by typically 1.6 [for $\phi(2170)$], 1.7 [for $X(4260)$], and 2.0 [for $Y_b(10890)$], compared to the ones calculated for the CDF and D0 at the Tevatron.

To estimate the number of events, we assume an integrated luminosity of 10 fb^{-1} at the Tevatron by the end

TABLE II. Cross sections (in units of pb) for the processes $p\bar{p}(p) \rightarrow \phi(2170)(\rightarrow \phi(1020)f_0(980) \rightarrow K^+K^-\pi^+\pi^-)$, $p\bar{p}(p) \rightarrow X(4260)(\rightarrow J/\psi\pi^+\pi^- \rightarrow \mu^+\mu^-\pi^+\pi^-)$, and $p\bar{p}(p) \rightarrow Y_b(10890)(\rightarrow Y(1S, 2S, 3S)\pi^+\pi^- \rightarrow \mu^+\mu^-\pi^+\pi^-)$, at the Tevatron ($\sqrt{s} = 1.96$ TeV) and the LHC ($\sqrt{s} = 7$ TeV and 14 TeV), using the MSTW PDFs.

	$\phi(2170)$	$X(4260)$	$Y_b(10890)$
Tevatron ($ y < 2.5$)	$2.3_{-0.9}^{+0.9}$	$0.23_{-0.05}^{+0.19}$	$0.0020_{-0.0005}^{+0.0006}$
LHC 7 TeV ($ y < 2.5$)	$3.6_{-1.4}^{+1.4}$	$0.40_{-0.09}^{+0.32}$	$0.0040_{-0.0011}^{+0.0013}$
LHCb 7 TeV ($1.9 < y < 4.9$)	$2.2_{-1.1}^{+1.2}$	$0.24_{-0.07}^{+0.20}$	$0.0023_{-0.0006}^{+0.0007}$
LHC 14 TeV ($ y < 2.5$)	$4.5_{-1.9}^{+1.9}$	$0.54_{-0.12}^{+0.44}$	$0.0060_{-0.0016}^{+0.0019}$
LHCb 14 TeV ($1.9 < y < 4.9$)	$2.7_{-1.6}^{+1.9}$	$0.31_{-0.11}^{+0.27}$	$0.0033_{-0.0010}^{+0.0011}$

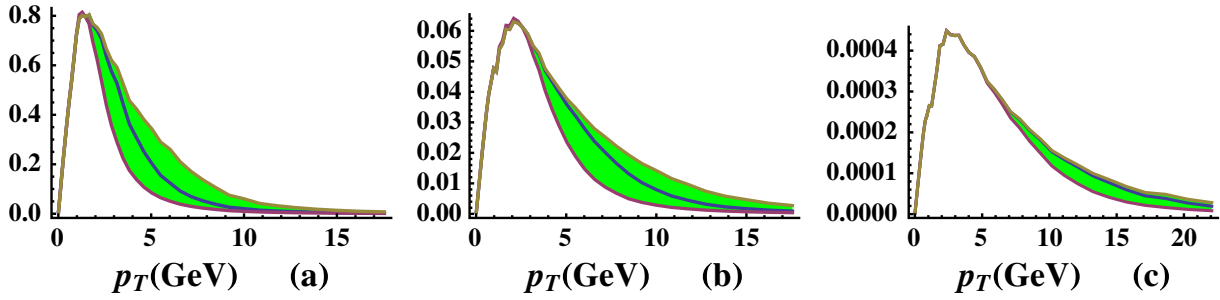


FIG. 2 (color online). Transverse momentum distributions $\frac{d\sigma}{dp_T}$ (in units of pb/GeV) for the process (a) $pp \rightarrow (\phi(2170) \rightarrow \phi(1020)f_0(980) \rightarrow K^+K^-\pi^+\pi^-) + \dots$, (b) $pp \rightarrow (X(4260) \rightarrow J/\psi\pi^+\pi^- \rightarrow \mu^+\mu^-\pi^+\pi^-) + \dots$, and (c) $pp \rightarrow (Y_b(10890) \rightarrow Y(1S, 2S, 3S)\pi^+\pi^- \rightarrow \mu^+\mu^-\pi^+\pi^-) + \dots$ at the LHC ($\sqrt{s} = 7$ TeV) with the rapidity cut $|y| < 2.5$ using the MSTW PDFs. Uncertainties caused by the matching functions are displayed through $1/[1 + (p_T/Q_{\text{match}})^4]$ with $Q_{\text{match}} = (2 \pm 1)m_V$.

of this year, and half that number at the LHC (for $\sqrt{s} = 7$ TeV) by the end of 2012. This yields 2.3×10^4 events for the mode $\phi(2170) \rightarrow \phi(1020)f_0(980) \rightarrow K^+K^-\pi^+\pi^-$, 2.3×10^3 events for the mode $X(4260) \rightarrow J/\psi\pi^+\pi^- \rightarrow \mu^+\mu^-$ [and approximately the same number for the $X(4260) \rightarrow J/\psi\pi^+\pi^- \rightarrow e^+e^-\pi^+\pi^-$ mode], and only about 20 events for the mode $Y_b(10890) \rightarrow Y(1S, 2S, 3S)\pi^+\pi^- \rightarrow \mu^+\mu^-\pi^+\pi^-$ [and approximately the same number of events for the $Y_b(10890) \rightarrow Y(1S, 2S, 3S)\pi^+\pi^- \rightarrow e^+e^-\pi^+\pi^-$ mode]. The corresponding numbers for the ATLAS and CMS [LHCb] are $1.8[1.1] \times 10^4$, $2.0[1.2] \times 10^3$, and $20[11]$, respectively. Hence, all these processes have measurable rates, given the luminosities at the Tevatron and the LHC, though the measurement of $Y_b(10890)$ in the Drell-Yan process may have to wait for higher luminosities and/or higher center-of-mass energy at the LHC.

In summary, we have presented the Drell-Yan cross sections and the corresponding differential distributions for the production of the $J^{\text{PC}} = 1^{--}$ exotic vector hadrons $\phi(2170)$, $X(4260)$, and $Y_b(10890)$ at the Tevatron and the LHC. The estimates given here are model independent due to the experimental input provided by the e^+e^- experiments. To unravel the dynamics underlying the exotic spectroscopy, one will have to undertake detailed dynamical studies involving the final states.

We acknowledge helpful discussions with Silja Brensing, Christian Hambrock, and Satoshi Mishima. W.W. is supported by the Alexander von Humboldt Stiftung.

*ahmed.ali@desy.de

†wei.wang@desy.de

- [1] For a recent experimental review, see A. Zupanc (Belle Collaboration), arXiv:0910.3404.
 [2] B. Aubert *et al.* (BABAR Collaboration), *Phys. Rev. Lett.* **95**, 142001 (2005).

- [3] Q. He *et al.* (CLEO Collaboration), *Phys. Rev. D* **74**, 091104 (2006).
 [4] C. Z. Yuan *et al.* (Belle Collaboration), *Phys. Rev. Lett.* **99**, 182004 (2007).
 [5] L. Maiani, V. Riquer, F. Piccinini, and A. D. Polosa, *Phys. Rev. D* **72**, 031502 (2005).
 [6] K. Nakamura *et al.* (Particle Data Group), *J. Phys. G* **37**, 075021 (2010).
 [7] B. Aubert *et al.* (BABAR Collaboration), *Phys. Rev. D* **74**, 091103 (2006).
 [8] M. Ablikim *et al.* (BES Collaboration), *Phys. Rev. Lett.* **100**, 102003 (2008).
 [9] C. P. Shen *et al.* (Belle Collaboration), *Phys. Rev. D* **80**, 031101 (2009).
 [10] N. V. Drenska, R. Faccini, and A. D. Polosa, *Phys. Lett. B* **669**, 160 (2008).
 [11] K. F. Chen *et al.* (Belle Collaboration), *Phys. Rev. Lett.* **100**, 112001 (2008).
 [12] I. Adachi *et al.* (Belle Collaboration), *Phys. Rev. D* **82**, 091106 (2010).
 [13] A. Ali, C. Hambrock, and M. J. Aslam, *Phys. Rev. Lett.* **104**, 162001 (2010).
 [14] A. Ali, C. Hambrock, I. Ahmed, and M. J. Aslam, *Phys. Lett. B* **684**, 28 (2010).
 [15] A. Ali, C. Hambrock, and S. Mishima, *Phys. Rev. Lett.* **106**, 092002 (2011).
 [16] A. D. Martin, W. J. Stirling, R. S. Thorne, and G. Watt, *Eur. Phys. J. C* **63**, 189 (2009).
 [17] H. L. Lai *et al.*, *Phys. Rev. D* **82**, 074024 (2010).
 [18] G. Altarelli, R. K. Ellis, and G. Martinelli, *Nucl. Phys.* **B143**, 521 (1978); **B146**, 544 (1978); *Nucl. Phys.* **B157**, 461 (1979).
 [19] J. Kubar-Andre and F. E. Paige, *Phys. Rev. D* **19**, 221 (1979).
 [20] J. C. Collins, D. E. Soper, and G. F. Sterman, *Nucl. Phys.* **B250**, 199 (1985).
 [21] R. P. Kauffman, *Phys. Rev. D* **44**, 1415 (1991).
 [22] G. A. Ladinsky and C. P. Yuan, *Phys. Rev. D* **50**, R4239 (1994).
 [23] M. Ablikim *et al.* (BES Collaboration), *Phys. Rev. D* **70**, 092002 (2004); **72**, 092002 (2005).